Supporting Information

Zhao et al. 10.1073/pnas.1719966115

Cell Lines and Reagents

Human HEI193 schwannoma cells (a gift from Xandra Breakefield, Massachusetts General Hospital) (1, 2) and mouse NF2$^{-/-}$ Schwann cells (3) were maintained in 10% Schwann cell medium containing Schwann cell growth supplement (ScienCell). Fluorescein *Lycopersicon esculentum* (tomato) lectin (FITC-lectin) was obtained from Vector Laboratories. CRZ was obtained from Selleck.

Ultrasound Measurement of Tumor Volume. Schwannomas were imaged using the VisualSonics Vevo 2100 In Vivo High-Resolution Micro-Imaging System (VisualSonics, Inc). Mice were placed in a prone position after being anesthetized with isoflurane, and aqueous ultrasonic gel was applied to the cranial window surface. A MS700 transducer with a frequency range from 30 to 70 MHz, providing an axial resolution of 30 μm with a 9-mm field of view, was clipped onto the 3D motor attached to the computer-controlled motor frame and positioned onto the cranial window surface for imaging of tumors. After locating the tumor region to the center of the image display, B-mode 3D image capture was enabled as per the manufacturer's instructions (4). Image frames were reconstructed into a 3D image, and the volume, consisting of multiple polygons, was calculated with Vevo 2100 software.

Gaussia Luciferase (Gluc) Assay of Tumor Growth. Both tumor cell lines were infected with lentivirus encoding secretive Gluc, and the measurement of plasma Gluc was performed as previously described (5–7). Briefly, 13 μL of whole blood was collected from a slight nick on tail veils and mixed with 5 μL of 50 mM EDTA immediately to avoid clotting. Blood samples were transferred to a 96-well plate, and Gluc activity was measured using a plate luminometer (GloMax 96 Microplate Luminometer; Promega). The luminometer was set to automatically inject 100 μL of 100 mM coelenterazine (Nanolight) in PBS, and photon counts were acquired for 10 s.

Infection of shRNA

The cMET shRNAi lentivirus was obtained from Sigma. NF2$^{-/-}$ cells (1×10^5 cells per well) were plated in flat-bottomed, 48-well plates. Lentiviral particles (multiplicity of infection = 5) and polybrene (8 μg/mL) were added into each well. The infected cells were selected with 0.5 μg/mL puromycin (8).

MTT Assay

One thousand cells were seeded into 38-mm^2 wells of flat-bottomed, 96-well plates in triplicate and allowed to adhere overnight, and 3-(4,5-dimethylthiazol-2-yl)-2,5-diphenyltetrazolium bromide (MTT; 5 mg/mL; Sigma Chemical Co.) was prepared in PBS. The number of metabolically active cells was determined by MTT assay (9).

Clonogenic Assay

Cells were seeded in triplicate in six-well plates and allowed to attach overnight, and they were treated with control IgG or B20 (100 μg/mL) the following day. After 48 h of treatment, cells were irradiated at room temperature using a conventional broad-field 250-kV X-ray machine (Stabilipan 2; Siemens). The dose rate was 1.77 Gy·min^{-1}. Cells were incubated for another 48 h, and the medium was changed every 2 d to allow colony formation. Two weeks later, cells were fixed with graded ethanol and stained with crystal violet [0.5% (wt/vol); Sigma]. Colonies of more than 50 cells were counted, and the surviving fraction (*SF*) was calculated by the following equation:

$$SF = \left(\frac{\text{no. of colonies formed after treatment}}{\text{no. of cells seeded}}\right) \Big/ \left(\frac{\text{no. of colonies formed in sham irradiated group}}{\text{no. of cells seeded}}\right). \quad [S1]$$

Histology and Immunohistochemistry

To evaluate HGF/cMET expression in human schwannomas, HGF (1:50; Abcam) and total and phosphorylated-cMET (pre-diluted and 1:200; Invitrogen) were stained in paraffin-embedded schwannoma tissues; paraffin sections with colon cancer were used as positive controls for HGF and cMET staining. Negative control slides (incubated with secondary antibody only) were included in all assays. The staining was scored by a pathologist as 0%, <10%, 11–50%, and 51–100%, and the intensity was scored as 0, weak (+1), moderate (2+), and strong (3+). To evaluate radiation-induced DNA damage, cells were cultured on glass coverslips and stained with γH2AX antibodies (1:400; Cell Signaling). Cells were judged as "positive" for γH2AX foci if they displayed 10 or more discrete dots of brightness. For quantitation of foci, a minimum of 300 cells was analyzed for each time point (10, 11). To evaluate tissue hypoxia, pimonidazole (50 mg/kg, i.p.) was injected 1 h before killing the mice. The tumor was harvested and fixed in 4% formaldehyde and embedded in paraffin blocks for sectioning (5 μm). The Hypoxyprobe Plus Kit (Hypoxyprobe) was used to detect the percentage of pimonidazole$^+$ area in the total viable tumor area (10, 12). To evaluate the proportion of perfused vessels, 50 μL of FITC-lectin (2 mg/kg) was injected into the tail vein of mice 10 min before euthanasia in order for lectin to circulate and bind to endothelial cells. Tumors were embedded in optimal cutting temperature (OCT) compound for cryosectioning (20 μm). Perfused vessels were fluorescently labeled by FITC, and CD31$^+$ staining demonstrated all microvessels in solid tumor. The percentage of FITC-lectin$^+$/CD31$^+$ vessels was quantified using ImageJ software (13). To evaluate tumor cell proliferation and apoptosis, slides were stained with proliferating cell nuclear antigen (1:1,000; Abcam) and TUNEL (ApopTag Peroxidase In Situ Apoptosis Detection Kit; EMD Millipore) following the manufacturers' instructions. Positively stained cells were manually counted. In brain slice culture, HLA staining (1:50; Abcam) was used to identify human tumor cells.

ELISA

Protein was extracted from snap-frozen tumors and diluted to a 2-μg/μL concentration according to protein assay. HGF protein level was quantified using a mouse HGF ELISA Kit (R&D Systems) following the manufacturer's instructions. Every sample was run in triplicate (14, 15).

Western Blot Analysis

Thirty micrograms of protein per sample was separated on 10% SDS-polyacrylamide gels as described elsewhere (8). Membranes were blotted with antibodies against cMet (1:1,000) and phospho-cMet (1:1,000), Stat3 (1:2,000) and phospho-Stat3 (1:1,000), Akt (1:1,000) and phospho-Akt (1:200), and Erk1/2 (1:1,000) and phospho-Erk1/2 (1:1,000). Antibodies were obtained from Cell Signaling (16). Densitometry of the bands was quantified using ImageJ.

Audiometric Testing

DPOAEs and ABRs were measured as described earlier (17). Briefly, animals were anesthetized via i.p. injection of ketamine (0.1 mg/g) and xylazine (0.02 mg/g). The tympanic membrane and middle ear were microscopically examined for signs of otitis media. All animals had well-aerated middle ears.

DPOAEs were recorded in response to two primary tones (f1 and f2) with the frequency ratio f2/f1 = 1.2 at half-octave steps from f2 = 5.66–45.25 kHz, while increasing intensity in 5-dB steps from a sound pressure level (SPL) of 15 to 80 dB. The 2f1/f2 DPOAE amplitude and surrounding noise floor were monitored, and the threshold was defined as the f2 intensity that created a distortion tone >0 dB of SPL.

ABRs were recorded between subdermal needle electrodes: positive in the inferior aspect of the ipsilateral pinna, negative at the vertex, and grounded at the proximal tail. The responses were amplified (10,000-fold), filtered (0.3–3.0 kHz), and averaged (512 repetitions) for each of the same frequencies and sound levels as used for DPOAE measurements. Custom LabVIEW software for data acquisition was run on a PXI chassis (National Instruments Corp.). For each frequency, auditory threshold was defined as the lowest stimulus level at which repeatable peaks could be observed on visual inspection. In the absence of an auditory threshold, a value of 85 dB was assigned (5 dB above the maximal tested level).

Tumor Material and Patient Characteristics

Clinical samples and data were used in accordance with a protocol approved by the Research Ethics Board at Beijing Tian Tan Hospital. All patients with NF2 were diagnosed according to the Manchester criteria. All tumor samples were obtained from patients during initial surgery, before any adjuvant therapy, at the Neurosurgical Department of Beijing Tian Tan Hospital. A diagnosis of schwannoma was established in all cases based on tumor histopathology. Gene expression analysis was performed on frozen tumor tissue samples, including 17 NF2 VSs and 10 sporadic VSs (Table 1). Four specimens of normal peripheral nerve were obtained post mortem and used as controls. An independent cohort of 29 paraffin-embedded samples collected from Beijing Tian Tan Hospital was analyzed by immunohistochemistry (Table 2). Stratification of patients according to tumor histology, stage, and grade was typical for a patient population diagnosed with NF2.

Gene Expression Analysis

VSs and normal nerve samples were analyzed on the Affymetrix Human Transcriptome 2.0 array. Sample library preparation, hybridization, and quality control were performed according to recommended protocols of Affymetrix. CEL files were imported into Affymetrix Expression Console (version 1.4), and gene level analysis (CORE content) was performed. Arrays were quantile-normalized (sketch) and summarized using the PLIER (Probe Logarithmic Intensity Error) algorithm with PMGCBG background correction. Probe sets were annotated according to the human genome build HG19 (GRCh37). Genes with a fold change ≥ 2 and $P < 0.05$ were selected for further analysis. Hierarchical clustering using the Pearson correlation metric (average linkage) was performed using the TM4 Microarray Software Suite (MeV v4.4; Dana–Farber Cancer Institute) (14).

To evaluate changes in mRNA level, qRT-PCR was performed using a SYBR Green-based protocol (14). All qPCR assays and analysis were performed on a Stratagene MX 3000 qPCR System operating MXPro qPCR software (Stratagene). The murine HGF mRNA primers used were as follows: forward primer, 5′-TTC CCA GCT GGT CTA TGG TC-3′; reverse primer, 5′-TGG TGC TGA CTG CAT TTC TC-3′.

Ex Vivo Culture of Human Tumors in Organotypic Brain Slice Culture

The CPA regions of mouse brain were sliced 300 μm thick. The brain slices were cultured in Millicell cell culture inserts in a six-well plate and incubated at 37 °C (18, 19). Fresh patient-derived VS and meningioma surgical samples were obtained following approval of the Partners Human Research Committee/Institutional Review Board, Massachusetts General Hospital. Under sterile condition, tumors were cut into 1 × 1-mm chunks using a biopsy punch needle (Miltex) and implanted into the brain slice. Two days later, CRZ (2 μM) was added into the culture medium and replaced each day. Fourteen days later, brain slices were fixed for histological staining and imaging analysis.

Statistical Analyses

Spearman's rho correlation coefficient was calculated. We determined whether growth curves significantly differed from each other by log-transforming the data, fitting a linear regression to each growth curve, and comparing the slopes of the regression lines (using an equivalent of ANOVA). Significant differences between two groups were analyzed using the Student's t test (two-tailed) or Mann–Whitney U test (two-tailed). All calculations were done using GraphPad Prism Software 6.0 and Microsoft Excel Software 2010. Differences in hearing response between multiple groups were evaluated with ANOVAs. Welch's t test was used for comparisons between two groups. The Benjamini–Hochberg correction for multiple comparisons was applied. HGF/cMET expression in patient schwannoma tissues was statistically analyzed using statistics software (Statistical Package for the Social Sciences Statistics, version 20.0; IBM) with an a priori significance level of $P = 0.05$. To evaluate synergy, we used Chalice Bioinformatics Software (chalice.horizondiscovery.com/documentation/analyzer/index.jsp) to calculate the Loewe excess. The correlation between clinical variables (tumor size, cyst, age at diagnosis, adhesion with brainstem, duration of symptoms) and the staining score of HGF and phosphor-cMET in NF2 schwannoma were analyzed using the Pearson correlation coefficient (r value).

1. Hung G, et al. (2002) Establishment and characterization of a schwannoma cell line from a patient with neurofibromatosis 2. *Int J Oncol* 20:475–482.
2. Prabhakar S, et al. (2007) Treatment of implantable NF2 schwannoma tumor models with oncolytic herpes simplex virus G47Delta. *Cancer Gene Ther* 14:460–467.
3. Wong HK, et al. (2010) Anti-vascular endothelial growth factor therapies as a novel therapeutic approach to treating neurofibromatosis-related tumors. *Cancer Res* 70: 3483–3493.
4. Sastra SA, Olive KP (2013) Quantification of murine pancreatic tumors by high-resolution ultrasound. *Methods Mol Biol* 980:249–266.
5. Chung E, et al. (2009) Secreted Gaussia luciferase as a biomarker for monitoring tumor progression and treatment response of systemic metastases. *PLoS One* 4: e8316.
6. Tannous BA (2009) Gaussia luciferase reporter assay for monitoring biological processes in culture and in vivo. *Nat Protoc* 4:582–591.
7. Kodack DP, et al. (2012) Combined targeting of HER2 and VEGFR2 for effective treatment of HER2-amplified breast cancer brain metastases. *Proc Natl Acad Sci USA* 109:E3119–E3127.
8. Liu J, et al. (2011) PDGF-D improves drug delivery and efficacy via vascular normalization, but promotes lymphatic metastasis by activating CXCR4 in breast cancer. *Clin Cancer Res* 17:3638–3648.
9. Xu L, Tong R, Cochran DM, Jain RK (2005) Blocking platelet-derived growth factor-D/platelet-derived growth factor receptor beta signaling inhibits human renal cell carcinoma progression in an orthotopic mouse model. *Cancer Res* 65:5711–5719.
10. Gao X, et al. (2015) Anti-VEGF treatment improves neurological function and augments radiation response in NF2 schwannoma model. *Proc Natl Acad Sci USA* 112: 14676–14681.
11. Floyd SR, et al. (2013) The bromodomain protein Brd4 insulates chromatin from DNA damage signalling. *Nature* 498:246–250.
12. Winkler F, et al. (2004) Kinetics of vascular normalization by VEGFR2 blockade governs brain tumor response to radiation: Role of oxygenation, angiopoietin-1, and matrix metalloproteinases. *Cancer Cell* 6:553–563.
13. Liu J, et al. (2012) TGF-β blockade improves the distribution and efficacy of therapeutics in breast carcinoma by normalizing the tumor stroma. *Proc Natl Acad Sci USA* 109:16618–16623.

14. Xu L, et al. (2009) Direct evidence that bevacizumab, an anti-VEGF antibody, up-regulates SDF1alpha, CXCR4, CXCL6, and neuropilin 1 in tumors from patients with rectal cancer. *Cancer Res* 69:7905–7910.
15. Xu L, et al. (2006) Placenta growth factor overexpression inhibits tumor growth, angiogenesis, and metastasis by depleting vascular endothelial growth factor homodimers in orthotopic mouse models. *Cancer Res* 66:3971–3977.
16. Xu L, Fukumura D, Jain RK (2002) Acidic extracellular pH induces vascular endothelial growth factor (VEGF) in human glioblastoma cells via ERK1/2 MAPK signaling pathway: Mechanism of low pH-induced VEGF. *J Biol Chem* 277:11368–11374.
17. Lysaght AC, et al. (2014) FGF23 deficiency leads to mixed hearing loss and middle ear malformation in mice. *PLoS One* 9:e107681.
18. Chadwick EJ, et al. (2015) A brain tumor/organotypic slice co-culture system for studying tumor microenvironment and targeted drug therapies. *J Vis Exp* e53304.
19. Chuang HN, et al. (2013) Coculture system with an organotypic brain slice and 3D spheroid of carcinoma cells. *J Vis Exp* 80:50881–50886.

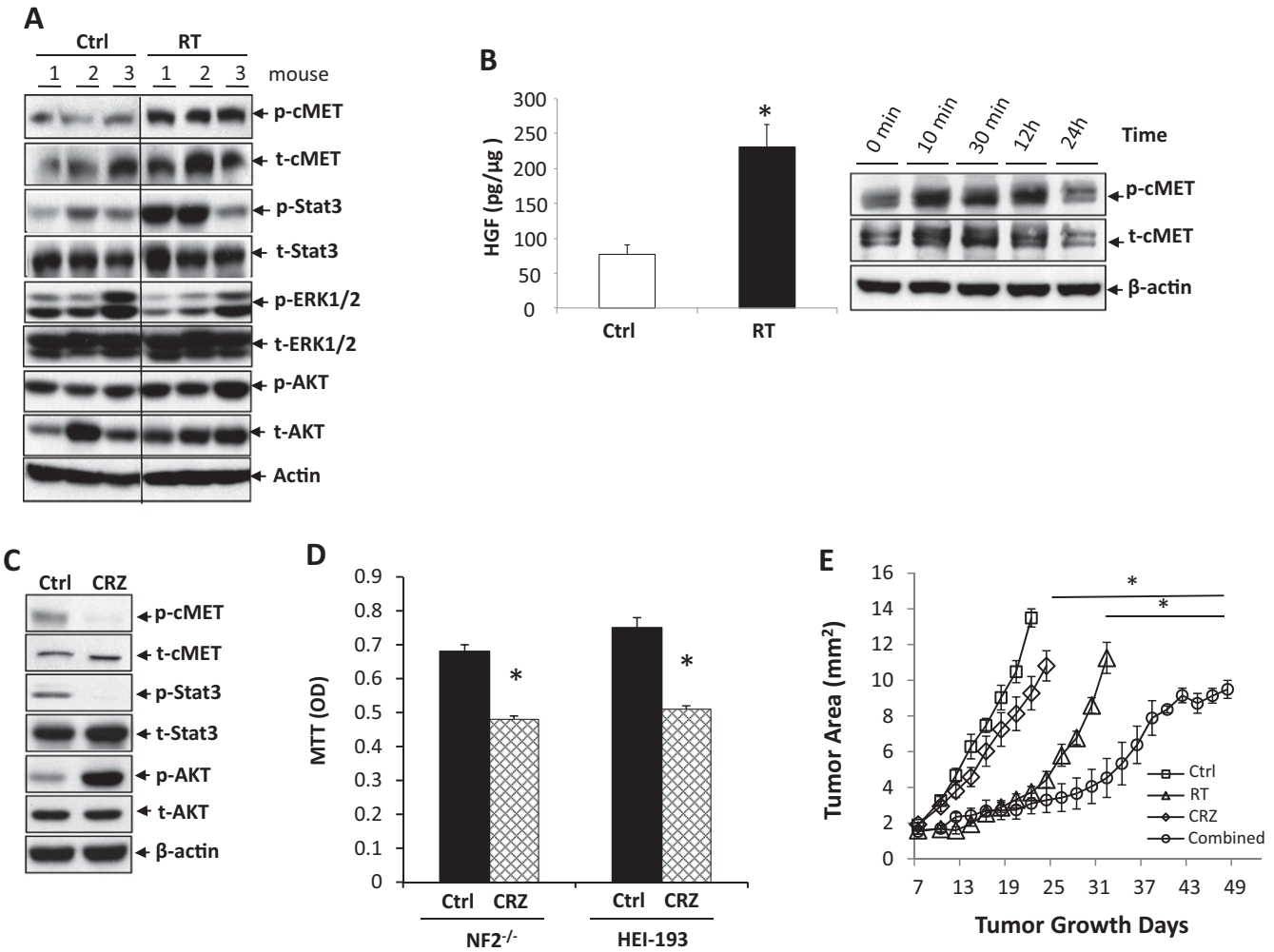

Fig. S1. RT activates and CRZ inactivates cMET signaling. (*A*) In the HEI-193 sciatic nerve model, when tumors reached 2.5 mm in diameter, mice were randomized into control (Ctrl) or radiation (5 Gy) groups. Mice were killed when tumors in the Ctrl group reached 1 cm in diameter. Protein samples were extracted ($n = 3$ for each group). The expression and activation of various signaling pathways were analyzed by Western blot analysis. p-, phosphorylation; t-, total expression. (*B*) Effect of radiation on HGF expression as assessed by ELISA and on p-cMET as assessed by Western blot in the HEI-193 cell line. (*C*) Effects of CRZ treatment (2 μM, 24 h) on the p-cMET and t-cMET and its downstream signaling pathways as assessed by Western blot analysis. (*D*) Effect of CRZ (2 μM) on $NF2^{-/-}$ and HEI-193 schwannoma cell viability as assessed by MTT assay. All assays were performed in triplicate. *$P < 0.05$ (Student *t* test). (*E*) HEI-193 tumor growth curve in the sciatic nerve model. Growth of Ctrl, CRZ-treated (50 mg/kg), 5 Gy irradiated (RT), and combined RT (5 Gy) and CRZ (Combined)-treated tumors was measured by Gluc level every 3 d. Data are representative of at least three independent experiments ($n = 8$), and are presented as mean ± SEM. *$P < 0.01$.

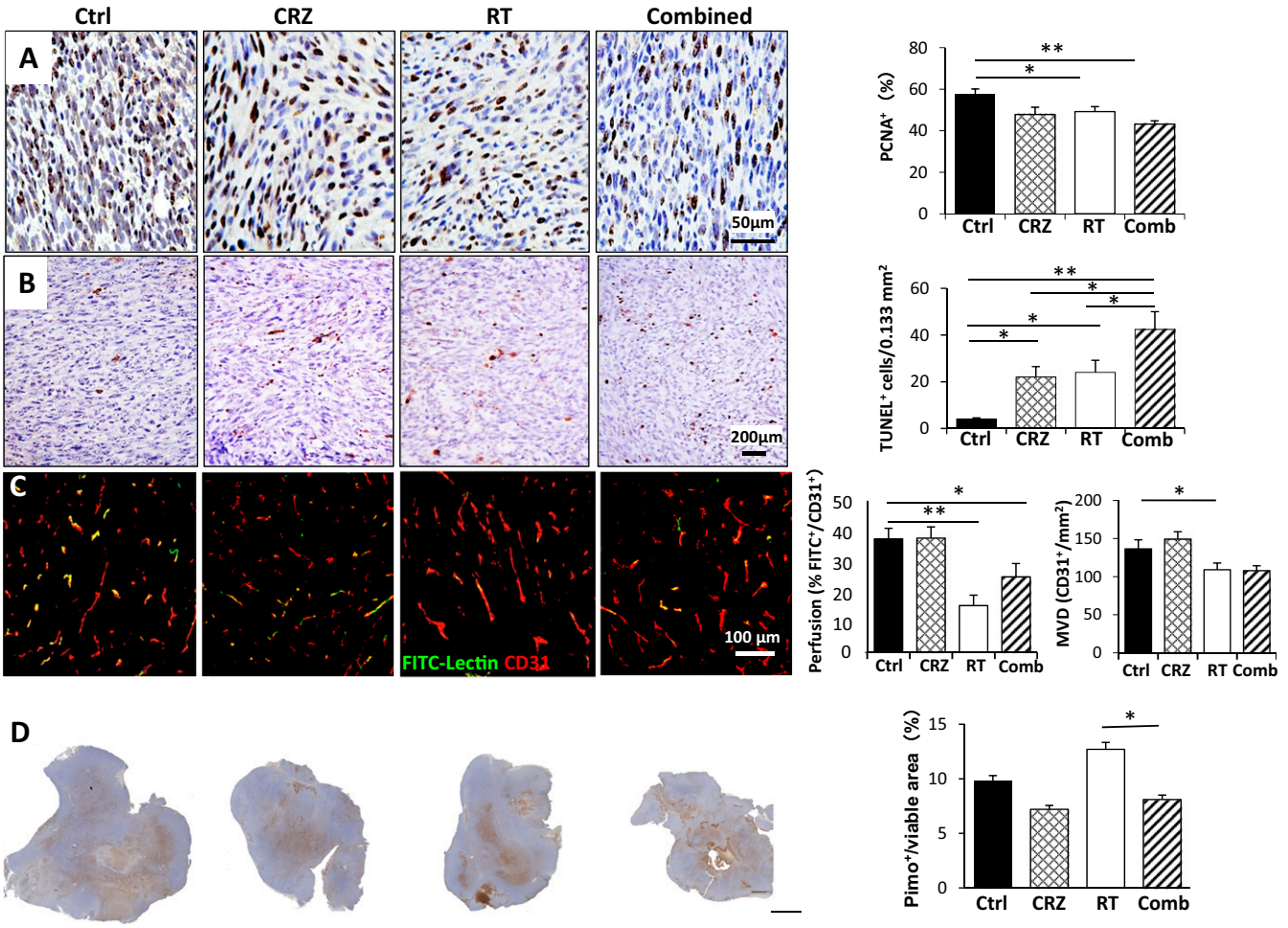

Fig. S2. CRZ treatment does not affect schwannoma blood vessel perfusion and tumor hypoxia. Representative staining images of immunohistochemistry staining and quantification of $NF2^{-/-}$ tumors in all treatment groups. (*A*) Proliferation [proliferating cell nuclear antigen (PCNA)]. (*B*) Apoptosis (TUNEL). (*C*) Fraction of perfused blood vessels (green, FITC-Lectin) among all vessels (red, CD31). Yellow, $CD31^+$ staining of perfused vessels. (*D*) Hypoxic fraction [pimonidazole $(Pimo)^+$, brown] of the viable nonnecrotic tumor tissue area. (Scale bar, 1 mm.) There were four mice per group, and 10 random fields were chosen for quantification. Data are presented as mean ± SD. $*P < 0.05$; $**P < 0.01$ (Student *t* test). Comb, combined RT and CRZ; Ctrl, control.

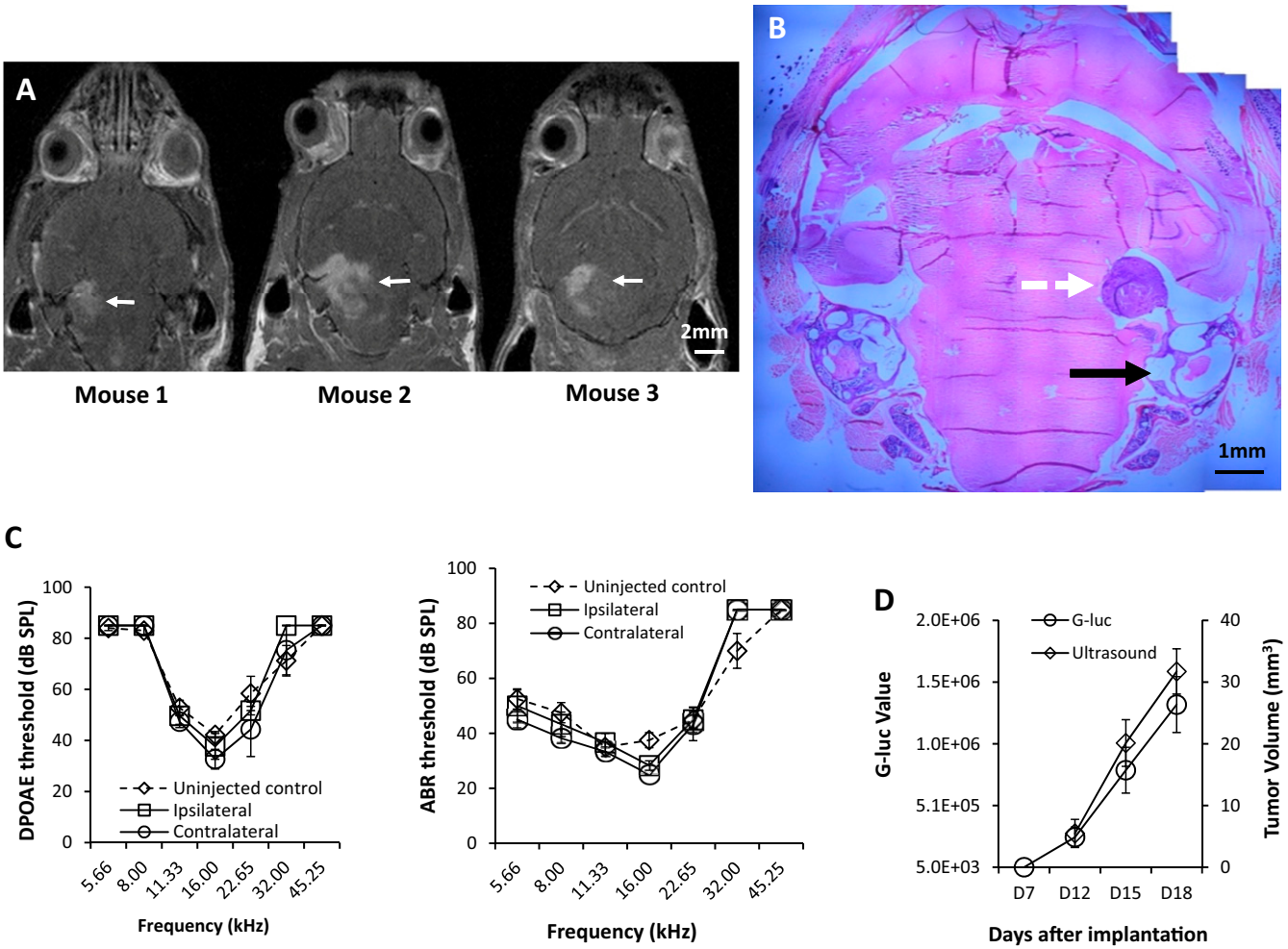

Fig. S3. Establishment of a schwannoma CPA model for evaluation of hearing function in mice. (*A*) Representative brain MR images of mice bearing $NF2^{-/-}$ tumors implanted in the CPA region ($n = 8$). White arrows point to CPA tumors. (*B*) Representative H&E images of the brain section of a mouse bearing $NF2^{-/-}$ tumors (white arrow) located in close proximity to the cochlea (black arrow). (*C*) DPOAE and ABR thresholds in uninjected control mice ($n = 4$) and in mice that underwent unilateral sham surgery (saline injection) ($n = 3$) and had hearing evaluated ipsilaterally and contralaterally. Data are presented as mean ± SEM. (*D*) Correlation of plasma Gluc value with tumor volume measured by ultrasound ($n = 12$).

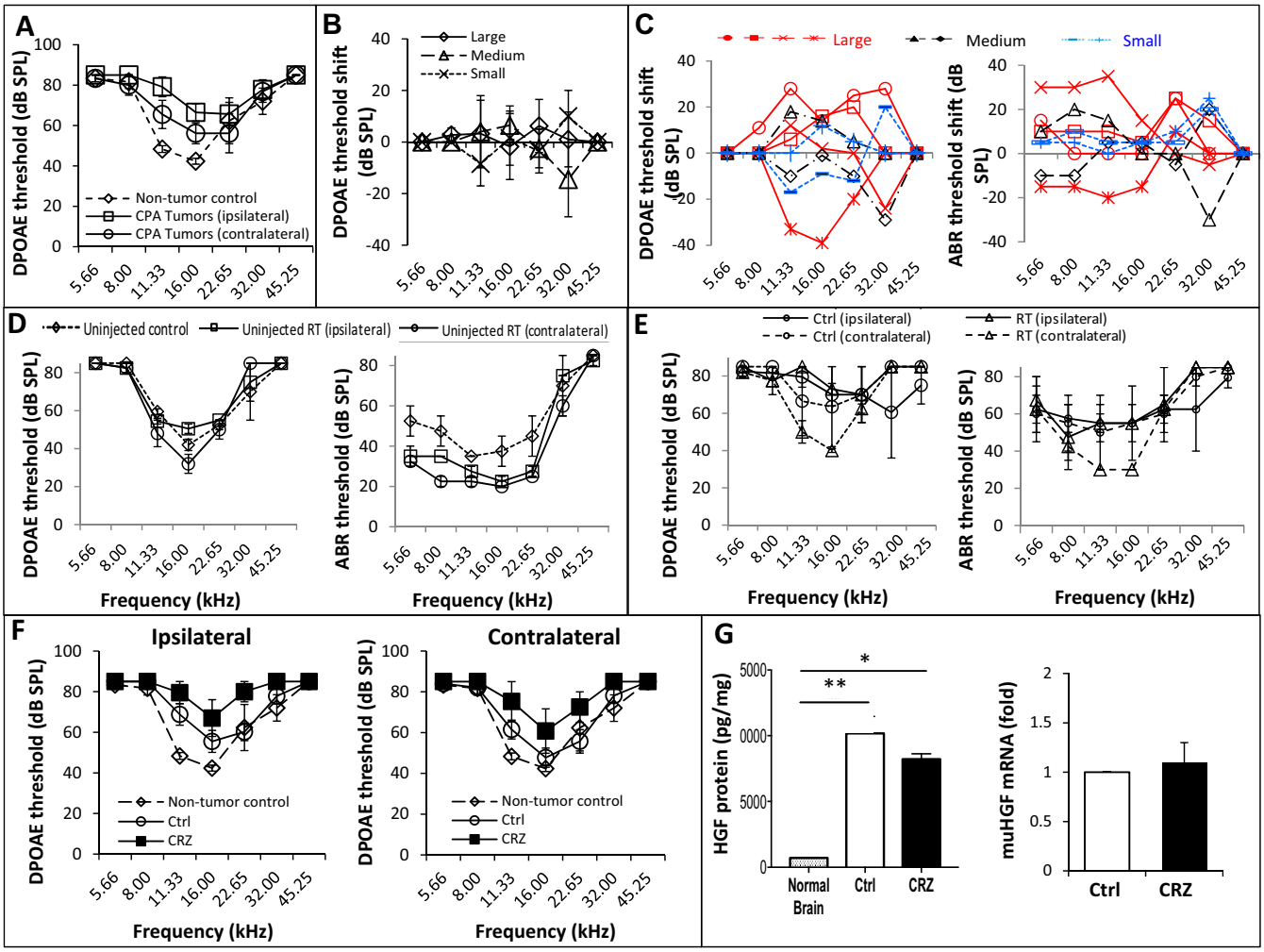

Fig. S4. Hearing tests in the CPA mouse model. (*A*) In mice bearing NF2$^{-/-}$ schwannomas in the CPA model ($n = 6$), the DPOAE threshold ipsilateral and contralateral to the tumor was compared with that in nontumor-bearing control mice ($n = 3$). (*B*) In the NF2$^{-/-}$ schwannoma CPA model, measurement of DPOAE threshold shifts (ipsilateral minus contralateral to the tumor) ($n = 8$ mice). There were two mice with a small tumor (Gluc $< 1.0 \times 10^5$ units, 10 mm^3), two mice with a medium-sized tumor (Gluc 1.0×10^5–3.0×10^6 units, 10–40 mm^3), and four mice with a large tumor (Gluc $> 3.0 \times 10^6$ units, >40 mm^3). (*C*) Individual DPOAE and ABR threshold shifts (ipsilateral minus contralateral side) for data presented in *B* and Fig. 4*B*. (*D*) In nontumor-bearing mice treated with control or radiation (10 Gy), measurement of DPOAE and ABR thresholds ipsilateral and contralateral to radiation. (*E*) In NF2$^{-/-}$ tumor-bearing mice treated with control (Ctrl; $n = 8$) or radiation (RT; 10 Gy, $n = 2$), measurement of DPOAE and ABR thresholds ipsilateral and contralateral to the tumor. (*F*) Measurements of DPOAE thresholds in non–tumor-bearing mice ($n = 3$) and in NF2$^{-/-}$ tumor-bearing mice of Ctrl ($n = 10$) and CRZ-treated ($n = 7$) groups ipsilateral and contralateral to the CPA schwannomas. $P = 0.1$ for 11.3 and 16.0 kHz, respectively. Data are presented as mean ± SEM. (*G*) Normal nontumor-bearing mouse brain and CPA tumors treated with Ctrl or CRZ were collected at an experiment end point. HGF protein level was measured by ELISA ($n = 3$ mice). *$P < 0.05$; **$P < 0.01$. mRNA level was measured by qRT-PCR. All assays were performed in triplicate.

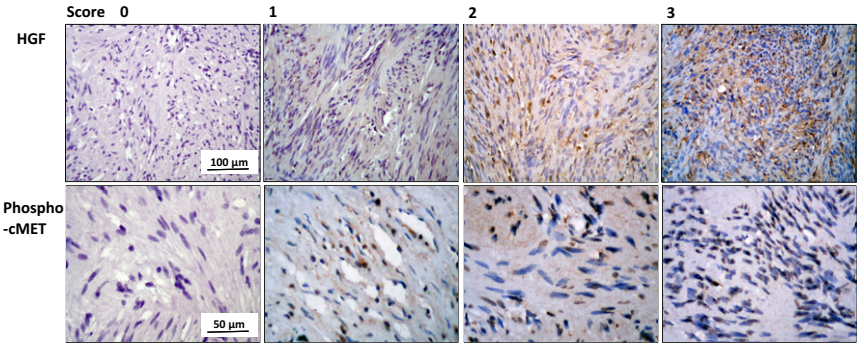

Fig. S5. IHC staining of HGF and cMET in human VSs. Representative HGF and phospho-cMET IHC-stained images of NF2-associated VS patient samples are shown. Tissue sections were stained with H&E and reviewed by a neuropathologist to confirm the presence and histology of schwannoma. Colon carcinomas were used as a positive control for HGF and phosphor-cMET staining. Negative control slides (incubated with secondary antibody only) were included in all assays. The staining was scored by a pathologist as follows: negative (0), weak (1), moderate (2), and strong (3) staining.

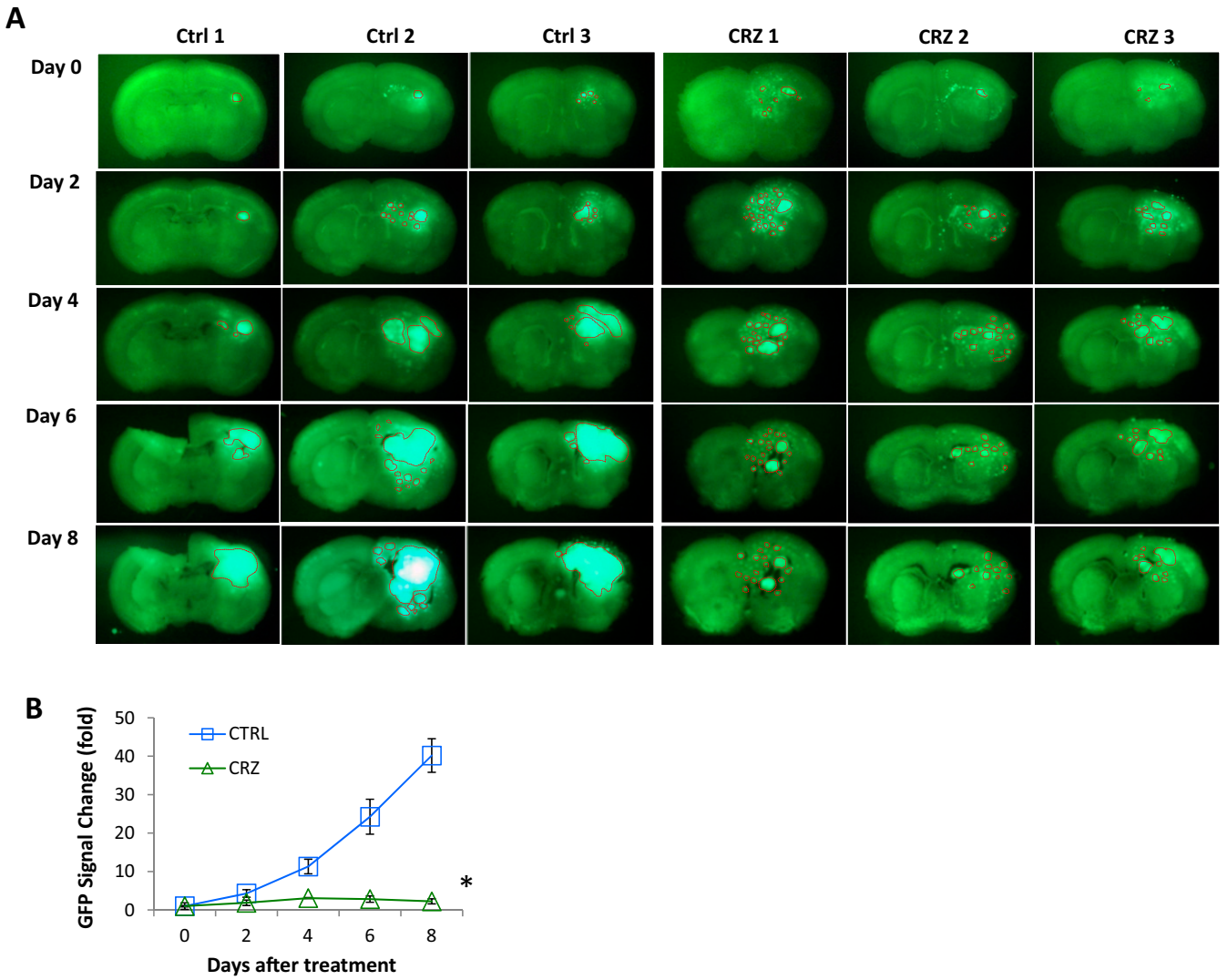

Fig. S6. cMET blockade inhibits the growth of $NF2^{-/-}$ schwannoma cells in the organotypic brain slice culture model. (*A*) Representative fluorescent images of cultured brain slices implanted with $NF2^{-/-}$ GFP cells (1,000 cells per slice) and followed for up to 8 d after no treatment [control (Ctrl)] or CRZ treatment (2 μM) ($n = 8$). (Magnification: 10×.) (*B*) Increase in tumor (GFP^+) area compared with day 0 after treatment, as quantified using ImageJ. *$P < 0.001$ (Student *t* test).